Received 28 May 2022, accepted 21 June 2022, date of publication 29 June 2022, date of current version 11 July 2022.

Digital Object Identifier 10.1109/ACCESS.2022.3187035

RESEARCH ARTICLE

Compact and Integrated Microstrip Antenna Modules for mm-Wave and Microwave Bands Applications

MARWA M. EL-WAZZAN, HUSSEIN H. GHOUZ, SHERIF K. EL-DIASTY, AND MOHAMED A. ABOUL-DAHAB, (Life Senior Member, IEEE)

Department of Communication and Electronics, Arab Academy for Science, Technology and Maritime Transport, Cairo 11799, Egypt

Corresponding author: Marwa M. El-Wazzan (engmarwawazzan@gmail.com)

ABSTRACT This paper presents two different antenna modules at two different bands with a compact size structure that is used for both of mm-Wave and microwave bands, with the objective of keeping the size as minimum as possible. The presented structure consists of two integrated modules with overall dimensions of $24 \times 15 \times 0.787$ mm^3 and is implemented on a Rogers RT5880 substrate. The first module is designed to resonate at 25.75 GHz with bandwidth of 4.15 GHz. The length of this module is taken as a constraint in designing the second module, which is the microwave one. This module is designed to have resonance frequency of 5.45 GHz with bandwidth of 1.12 GHz. The two modules are etched on the same substrate in an integrated fashion to give the required structure with two separate feeds and a separation gap between them in the ground plane. The proposed antenna structure is simulated using the CST-MW studio simulator, where it is found that for the mm-Wave module, the band's gain is 5.58 dBi and the efficiency is 0.87 at 25.75 GHz. As for the microwave module, the gain is 2.45 dBi and the efficiency is 0.77 at 5.45 GHz. The proposed structure is implemented practically and the relevant measures agree with the simulated ones. A comparison of the proposed structure with other designs available in literature shows that it exhibits the minimum size among them, while keeping the other parameter values of comparable orders. The proposed structure is suitable for being used in 5G applications where both of the microwave and millimeter- wave bands are utilized.

INDEX TERMS Microstrip antenna, dual-band antenna, fourth-generation (4G), mm-Wave fifth generation (5G), DGS.

I. INTRODUCTION

The fifth generation (5G) wireless communication systems was developed to cope with the modern wireless devices requirements which the fourth-generation (4G) could not handle. The most critical characteristics of 5G are high data rate, high capacity, high reliability, and low latency [1]–[3]. Since current devices are unable to meet the demands of 5G, new devices with new designs and features need to be developed. The antenna characteristics are considered among the most prominent features of the new designs [4], [5]. However, there are many challenges that face the design of antennas suitable for 5G applications. Among these are the variety of the utilized bands, beam scanning capability with wide angles, ultra-wideband circularly-polarized antenna elements, high-gain, and low-profile in addition to the possibility of being manufactured at low-cost [6].

To handle the excessive number of expected users, the allocated spectrum of the 5G is extended to reach the millimeter wave bands [7]. This will make it necessary to introduce mobile devices that can operate in dual widely separated frequency bands.

The problem of designing an antenna that can cope with very widely separated bands is dealt with through three different approaches. The first one is to design a single-port fractal antenna module that works in the microwave and mm-Wave

The associate editor coordinating the review of this manuscript and approving it for publication was Wendem Beyene.

5G bands at the same time along with band-pass filter. The second approach is to design a single port dual-band patch antenna that works in both of the microwave mm-Wave 5G band. The third approach is to design two different antenna modules at two different bands with two separate ports that operate simultaneously in an independent manner in both microwave and mm-Wave 5G bands.

As far as the first approach is concerned, monopole antennas with fractal geometries were proposed. The authors in [8] proposed a patch that incorporated printed star-triangular fractal microstrip-fed monopole antenna with a semielliptical ground plane. The antenna covered the frequency band from 1 to 30 GHz continuously with a compact size of 20×20 mm^2. In [9] a compact monopole antenna using fractal geometries was proposed with bandwidth extending from 3 to 26 GHz with a bigger size of 22×33.4 mm^2. A staircase fractal curve was applied on a microstrip line which fed a truncated corner square patch antenna. This configuration was proposed by the authors in [10], where the band 0.1GHz – 30 GHz was continuously covered, with a size area of 60×60 mm^2. In [11], the authors presented a geometrical structure that incorporated a combination of the Peano-Gosper, Koch and Minkowski fractal curves. It covered a frequency range 1-20 GHz with maximum gain of 5.08 dBi at 3.4 GHz. This antenna occupied a size area of 50×50 mm^2.

The key issue with this first approach was the continuous bandwidth, which necessitated the addition of new measures to the main design in order to eliminate unnecessary resonance frequencies and increase antenna efficiency while lowering losses. This approach's complicated architectures and repetitive steps were also a concern [12], [13].

As for the second approach, it was based upon a single port patch antenna that could work in both microwave and mm-Wave 5G bands. A compact Phi-shaped monopole antenna derived from the conventional elliptical monopole for super wideband applications was proposed in [14]. The use of quarter elliptical ground plane allowed merging of the distinct bands resulting in a single continuous band from 3.8 to 38 GHz. In [15] the authors proposed a patch antenna that utilized the photonic- band gap (PBG) to operate in the 5G microwave band (3.1-3.5 GHz) and 5G mm-Wave band (24-27 GHz) through a switching technique. The achieved gain had a peak value of 9.46 dBi, but with a large size of 44×48 mm^2. A single-fed 4G/5G multiband antenna was presented in [16], where Franklin strip monopole antenna was designed to cover the 2.4 and 5.5 GHZ bands, while a rectangular patch was designed to cover the 28 GHz band. The antenna had peak gain of 7.35 dBi and moderate size of 35×45 mm^2. Although this structure offered continuous bandwidth coverage with a simple design, the moderate gains with moderate size in a single design were not achieved simultaneously. The authors in [17] presented a single port antenna composed of a monopole patch to cover the microwave band (2.7 – 7.9GHz) in addition to a patch array to cover the mm-Wave band (58.6 – 61.3 GHz) with maximum gains reaching 5 dBi and 12.5 dBi, respectively. This antenna had a large size of 40×50 mm2. This technique had numerous drawbacks that ought be addressed, such as the large size of most of its designs, in the existence of cross polarization, the complexity of the design, in addition to requirement for a filter in most circumstances [15].

The third approach was based upon designing two separate antennas one for the microwave and the other for mm-Wave 5G bands, then integrating both in one structure. The idea of a dual-band monopole MIMO antenna combined with a tapered slot antenna array (TSAA) for 4G/5G mobile devices was presented in [18]. The proposed structure used the geometry of 2-element monopole MIMO to cover the microwave 5G frequencies. An end-fire antenna array was added to cover the high frequencies of 5G. This structure provided high isolation (more than 25-dB) while achieving a high gain of 15 dBi at the mm-Wave band. However, the size was considerably big (70×50 mm$^{2)}$. The authors in [19] presented a structure composed of a 4G MIMO antenna that was combined with a mm-Wave 5G slot antenna array with an overall size of 60×100 mm^2. The MIMO antenna had a resonance frequency of 2160 MHz and mild isolation (more than 15 dB), while the mm-Wave 5G antenna array had a resonance frequency of 27.6 GHz and high isolation from the 4G MIMO antennas (more than 25-dB). In [20], the authors proposed an integrated MIMO scheme suitable for (4G) and mm-Wave (5G) wireless applications and relevant handheld devices. It comprised a two-element array for the 4G band and another two-element array for the 5G one with Defected Ground Structure (DGS). This design had an overall size of 110×75 mm^2 and was capable to resonate at 3.8, 5.5 and 26.85 GHz with peak gain of 10.29 dBi. The isolation was found to be about 43 dB for both microwave and millimeter-wave band. In [21], the authors proposed a corner-bent structure to achieve high isolation between the antenna modules incorporated. The proposed structure comprised a 4G LTE MIMO module composed of two-element microstrip-fed slot antennas that operated at the 1.7-3GHz band, in addition to a MIMO module composed of two element wideband tapered slot antennas that operated at the 25-38 GHz band. The structure had the size of $30 \times 14 \times 0.254$ mm$^{3\cdot}$ The corner- bent approach was also adopted by the authors in [22] to design an LTE - mm-Wave 5G dual band antenna configuration. The proposed configuration was composed of two geometrically perpendicular arms with a bent substrate, one for the LTE band (2.5-3.5 GHz) and the other for the 5G band (28 GHz). The arm sizes were $63 \times 5.6 \times 0.5$ mm^3 and $28.3 \times 5.6 \times 0.5$ mm^3 respectively, and the coupling between them was less than 25 dB. However, still there is a need for new designs with smaller dimensions to cope with the miniaturized portable 5G devices. All of the designs listed above still had comparably larger sizes for being utilized in miniaturized terminal equipment that operate in dual band (e.g. 5G applications). Still there is a need for simple and smaller sizes dual band antennas without degrading the performance metrics. Realizing higher performance metrics as Gain, efficiency and VSWR) is also a challenging issue.

In this paper, an antenna structure that is capable of operating in both of the mm-Wave and microwave bands of the 5G is introduced. The proposed structure incorporates two antenna modules with two separate ports: one is operating at the 5G mm-Wave band while the other is operating at the 5G microwave one. The objective of the proposed designs is to build an integrated structure that comprises two different antenna modules operating at two different frequency bands. The integrated structure is designed so as to attain the compacted possible dimensions, while not sacrificing the performance measures (e.g. gain, efficiency, etc.).

The main contributions of this paper are as follows:

1- Proposing a patch antenna module that resonates at 26 GHz (mm-Wave band). The design is based on a circular patch that is fed from a tapered feedline. To facilitate control of the resonance frequency, slots and slits are introduced. To allow the module to resonate at the required frequency with a smaller size patch, an elliptically shaped DGS is introduced.
2- Under the length constraint of the previously proposed mm-Wave module, a microwave patch antenna module is designed to resonate at 5.4 GHz. The design is based upon an H-shaped patch with insets and slots to facilitate control of the resonance frequency. In order to come down to the required resonance frequency, an elliptically shaped DGS is introduced.
3- The proposed two modules are incorporated in one structure with two opposite and separate feeds. To eliminate coupling between the two modules, an isolation gap of a suitable width is introduced in the common ground plane between the two modules.

The paper is organized as follows. The methodology of antenna design is clarified in section II. The antenna configuration and the design steps for all of the mm-Wave, microwave 5G bands antennas and the two compact and integrated microstrip antenna modules are discussed in Section III. The practical measurements are presented in Section IV. Finally, Section V brings the paper to a close in the conclusion.

II. METHODOLOGY

The methodology adopted here is based upon designing two separate patch antenna modules; one operates in the mm-Wave band and the other in the microwave band. The two modules are then combined in one structure. In each of them, we start to design a patch that resonates at a higher frequency than the required one (f_r), and then by introducing a patch-insets and a patch-slots, along with a ground-slots (DGS), the resonance frequency is reduced to the desired one (f_r). In fact, this approach reduces the overall dimensions of the designed module.

The sequence followed is to first design the mm-Wave band antenna module. This antenna is designed as a tapered feedline circular patch with insets, circular slot, and DGS. The parameters of this antenna are adjusted to allow it to resonate at 25.75 GHz with gain of 5.58 dBi and overall size 15 × 6 mm^2. Secondly, the other antenna module that operates at the microwave band of the 5G is designed. This module is designed under the length constraint of 15 mm, which is the same length of the first antenna module so as to facilitate combining it with the mm-Wave module in one structure. The second antenna module is a modified version of the H-shaped patch [23] with its size selected to allow it to resonate at higher mm-Wave band (above 32.0 GHz). Then, it is customized so to be able to resonate at the lower microwave desired frequency by adding edge slots, insets, and DGS. The proposed antenna module resonates at 5.45 GHz with overall size 15 × 16 mm^2. Finally, the proposed antenna structure is formed by combining and etching the two antenna modules on the same substrate with an inter-gap (2.0mm) between them in the common ground plane. This is smallest gap width that achieves an acceptable value of isolation between them (more than 25-dB).

The proposed designs and relevant simulation results are carried out using CST_MW Studio platform. The proposed designs as well as the final integrated one are practically implemented and tested. Measured and simulated results are compared to each other, and also compared with similar designs available in literature

III. PROPOSED DESIGN

A. MM-WAVE ANTENNA MODULE

1) DESIGN STEPS

In this section, we use the circular geometry to take the advantage of the small size [24]. It has another important advantage as it is easier to achieve the best impedance matching in the mm-Wave bands [25].

The design is carried out through a number of steps, with relevant results that are carried out using the CST_MW Studio simulator. These steps are shown in Figure 1 with the implementation steps illustrated in Figure 1(a) and the relevant reflection coefficients plotted versus frequency in Figure 1 (b).

The design starts with a circular patch with tapered feedline [26] as a first step. To design a circular patch in that resonates at a certain frequency, we follow these equations given [27] to get the required radius as follows:

$$a = \frac{F}{\left\{1 + \frac{2h}{\pi \varepsilon_r F}\left[\ln\left(\frac{\pi F}{2h}\right) + 1.7726\right]\right\}^{1/2}} \tag{1}$$

where

$$F = \frac{8.791 \times 10^9}{f_r \sqrt{\varepsilon_r}}$$

The feed line width (W_f) is calculated as follows [28]:

$$\frac{W_f}{2} = \frac{8e^A}{e^{2A} - 2} \tag{2}$$

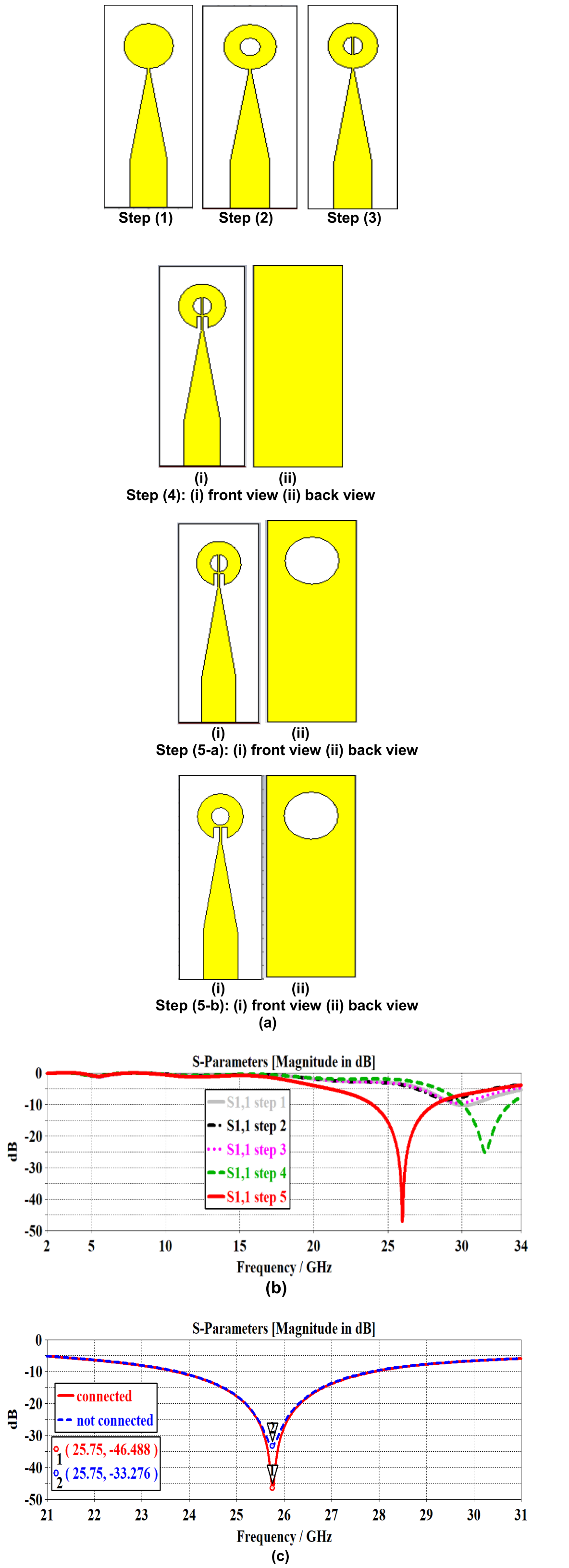

FIGURE 1. **Design steps of the mm-Wave antenna module (a) Implementation steps (b) Return loss at each design steps (c) Return loss of design step 5-a and 5-b.**

when

$$\frac{W_f}{2} \leq 2$$

$$\frac{W_f}{2} = \frac{2}{\pi}\{B-1-\ln(2B-1) + \frac{\varepsilon r-1}{2\varepsilon r}\left[\ln(B-1)+0.39-\frac{0.61}{\varepsilon r}\right]\} \quad (3)$$

when

$$\frac{W_f}{2} \geq 2$$

where;

Z_0 is the characteristic impedance of transmission line, εr is the Effective dielectric constant,

$$A = \frac{Z_0}{60}\sqrt{\frac{\varepsilon r+1}{2}+\frac{\varepsilon r+1}{\varepsilon r-1}(0.23+\frac{0.11}{\varepsilon r})} \text{ and } B = \frac{377\pi}{2Z_0\sqrt{\varepsilon r}}$$

The tapered feeding is found most suitable since both the feed-line and the patch are approximately of the same width. The dimensions of the patch in this step are selected to allow it to resonate at 30 GHz. However, this frequency is higher than the required one (25.75 GHz). In order to reduce the resonance frequency, we modify the construction of the patch by adding a circular slot as a second step. Although the introduction of this slot results in changing the current distribution on the patch, the resonance frequency is slightly lowered. In step 3, a connecter is added at the middle of the slot, with two slits introduced at both sides. Although this results in lowering the return loss more significantly, the resonance frequency is increased to reach 32 GHz. To allow the patch to resonate at a lower frequency, we introduce an elliptically-shaped DGS as a final step (shown in Figure 1(a) step 5-a). A parametric study is carried out to select the appropriate dimensions of the DGS so as to allow the module to resonate at the required frequency (25.75 GHz). The effect of the connector in the middle of the slot in the presence of the DGS is illustrated by comparing the return loss of the design in step 5-awith that when there is no middle connector as illustrated in design step 5-b. As shown in Figure 1(c), the return loss is lowered more significantly in the presence of the connector in the middle of the slot.

The proposed design of the mm-Wave patch antenna module is shown in Figure 2. Table 1 illustrates the front view dimensions of the designed microwave band patch antenna module, while table 2 illustrates back view dimensions of the module.

2) SIMULATION RESULTS

Figure 3 illustrate the frequency response of the gain, efficiency and VSWR respectively. It is clear that the gain is 5.58 dBi, efficiency is 0.87 and the VSWR value is 1.008 at 25.75 GHz. In all of these curves, it is obvious that the optimum values are obtained at nearly the same required frequency.

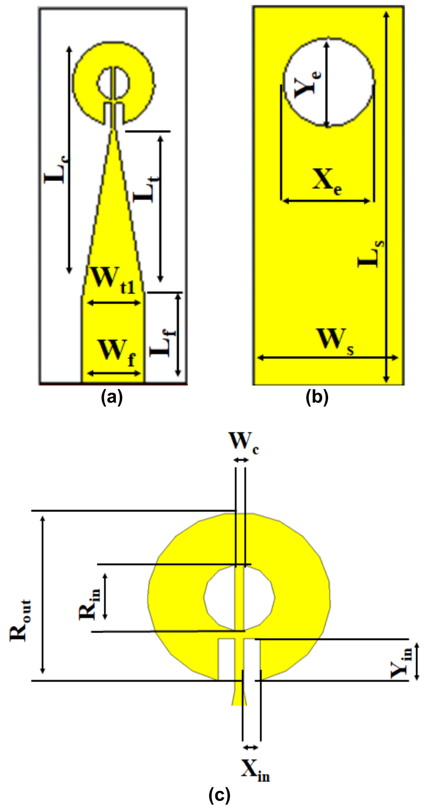

FIGURE 2. The proposed design of the mm-Wave patch antenna module (a)Front view (b) back view (c) details of the circular patch.

TABLE 1. Front view dimensions of the designed mm-wave patch antenna module.

	Width (in mm)		Length (in mm)	
	Symbol	Value	Symbol	Value
Patch	R_{out}	3.34	R_{out}	3.34
Slot	R_{in}	1.3	R_{in}	1.3
Feed-line	W_f	2.519	L_f	3.5
Tapper	W_{t1} / W_{t2}	2.519	L_t	6.665
Left insect	X_{in}	0.3	Y_{in}	0.8
Right insect	X_{in}	0.3	Y_{in}	0.8
Connect	W_c	0.1679333	L_c	9.25

TABLE 2. Back view dimensions of the proposed mm-wave patch antenna module.

	width (in mm)		Length (in mm)	
Ground	W_s	6	L_s	15
DGS	Major axis		Minor Axis	
	X_e	3.64	Y_e	3.5

The radiation pattern at the frequencies 23.7, 25.75 and 27.7 GHz (which are within the bandwidth) are shown in Figure 4 (a) in E- and H- planes. In the H-plane when $\varphi = 0^o$, it has an omnidirectional pattern. The E-plane when $\varphi = 90^o$ has one deep null at $\theta = -90^o$ for all of the measured frequencies and another non-deep null appears at $\theta = 60^o$ in case of f = 25.7 GHz. So, it could be considered a quasi- omnidirectional pattern in the mm-Wave band. The 3-D pattern at 26 GHz is shown in Figure 4 (b)

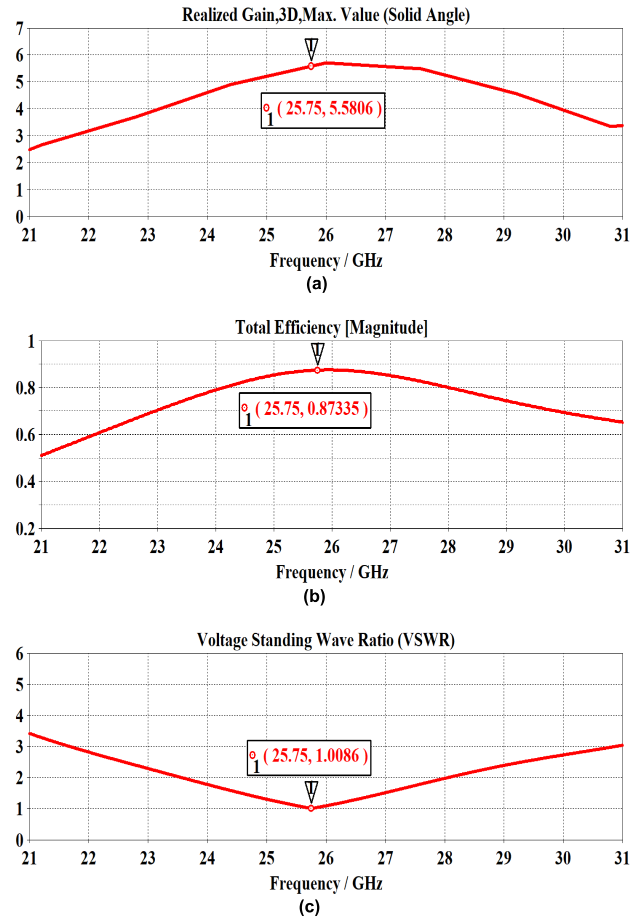

FIGURE 3. Frequency response of the of the designed mm-Wave 5G band (a) antenna Gain (b) Efficiency (c) VSWR.

As shown in Figure 4(a) the gain is nearly the same at the three frequencies, namely 23.7 GHz, 25.7 GHz and 27.7 GHz (within 1.3 dB). This is in agreement with the results given in the diagrams shown in Fig. 3(a).

Table 3 gives a comparison between the parameter values of the proposed mm-Wave patch antenna and other different designs available in literature. The proposed design has the smallest width of 6 mm. It is quite notable that the other parameters are of comparable values with those of other available designs. Moreover, the proposed design exhibits the highest return loss among the other designs

B. MICROWAVE BAND ANTENNA MODULE

1) DESIGN STEPS

Here, a rectangular patch is selected for the design. The principal constraint in the design is the length of the module

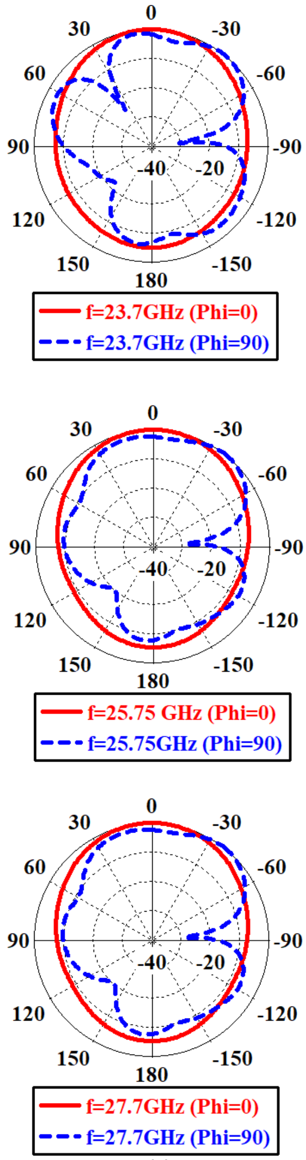

(a)

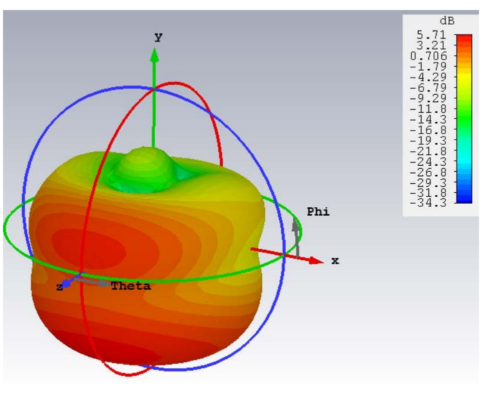

(b)

FIGURE 4. The radiation pattern of the proposed mm-Wave antenna module (a) E and H plane patterns at different frequencies (b)The 3-D radiation pattern at 26 GHz.

TABLE 3. Comparisons between the parameter values of the proposed mm wave patch and different designs available in literature.

Parameter Ref. No.	Resonance frequency (GHz)	Size (mm)	Gain (dBi)	BW (GHz)	Return loss (dB)
[29]	26	13.1 × 17.9	7.41	4.788	-35.66
[30]	23.1, 28	9.1 × 9	3.94 3.76	7.7	-40 -40
[31]	28.5	6 × 6	10	1.637	-32.86
[32]	28	8 × 10	3.95	8	-37
Proposed	25.75	6 × 15	5.58	4.15	-47.65

which should not exceed that of the previously designed mm-Wave one. This constraint necessitated designing a patch that resonates at higher frequency (13 GHz) than the required microwave one. However, the use of an ordinary ground plane permits the patch to resonate at other two frequencies as a result of other modes. To lower the resonance frequency, edge slots and slits are introduced to the patch. By introducing DGS, we can change the current distribution on the patch, allowing lowering the resonance frequency [33]. The DGS also has the advantage of preventing the unwanted resonance frequencies in the mm-Wave bands. Moreover, elliptically shaped DGS allow this patch to resonate at the required microwave band. The patch with the selected DGS gives the required microwave band module.

The designed module is based upon a shaped rectangular patch antenna with two edge slots and two insets (H-shaped) with elliptically-shaped DGS. In order to reach the final design, we have gone through several steps that are simulated using the CST_MW Studio platform.

The design steps are shown in Figure 5(a) while the plots of relevant return loss at all the steps are shown in Figure 5 (b). We start the first step by considering a conventional rectangular patch to resonate at 13GHz. The corresponding width (W_p) and length (L_p) are obtained according to [27] as follows:

$$W_p = \frac{\lambda_o}{2\sqrt{0.5(\varepsilon_r + 1)}} \tag{4}$$

where λ_o is the wavelength in the free space and ε_r is dielectric constant of the substrate.

$$L_p = L_{eff} - 2\Delta L \tag{5}$$

where Effective length (L_{eff}):

$$L_{eff} = \frac{C}{2f_r\sqrt{\gamma_{eff}}}$$

Length extension (ΔL):

$$\Delta L = 0.412h\frac{(\varepsilon_{eff}+0.3)\left(\frac{W}{H}+0.264\right)}{(\varepsilon_{eff}-0.258)\left(\frac{W}{H}+0.8\right)}$$

However, as shown in Figure 7 (b), the viewed band also has a lot of wobbles. The second step is adding two insets

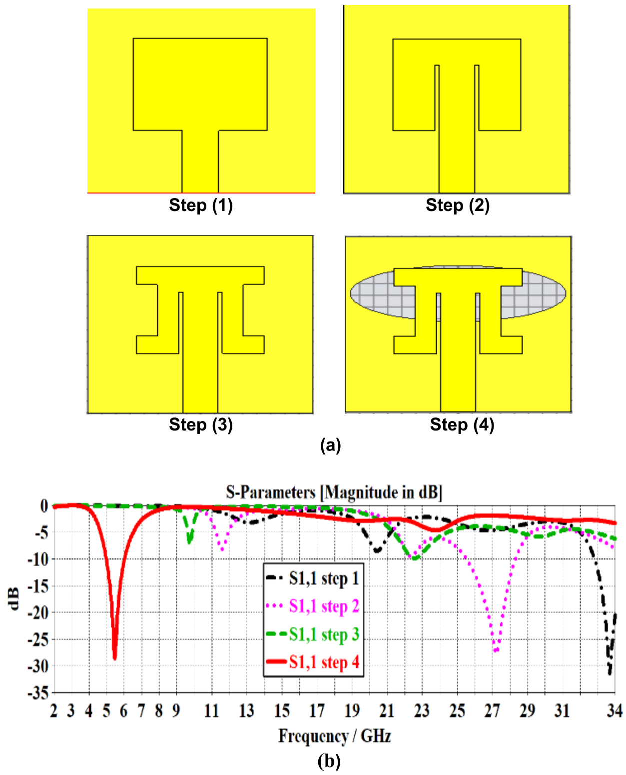

FIGURE 5. Design steps of the microwave antenna module (a) Implementation steps (b) Reflection coefficient at each design steps.

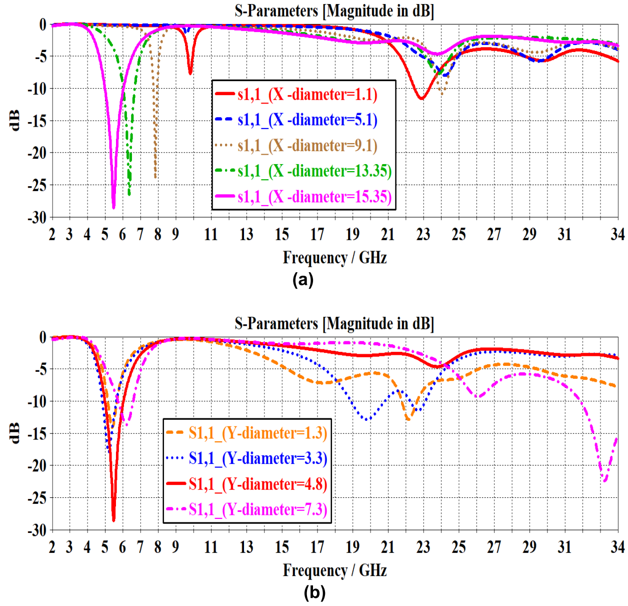

FIGURE 6. Return loss plot in accordance with the parametric study of the elliptically shaped DGS dimensions (X_e and Y_e) (a) Major axis (X) (b) Minor axis (Y).

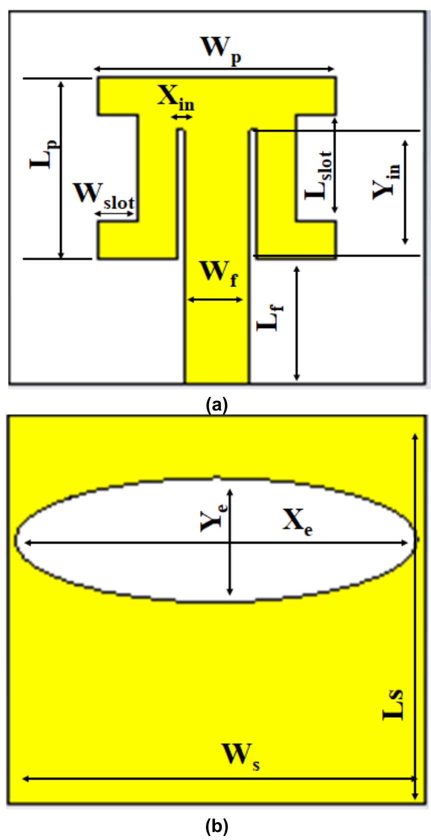

FIGURE 7. The proposed design of the microwave patch antenna module (a) Front view (b) back view.

to the patch. Such insets results in lowering the resonance frequency to a value which is around 11.5 GHz. The next step is to add the edge slots to the patch so as to take the H-shape. We note in Figure 7(b) that several nulls appear, one of which is at nearly double the value of the required one. The last step is to introduce an elliptically-shaped DGS to the design to lower the resonance frequency.

A parametric study is carried out to select the appropriate dimensions of the elliptically-shaped DGS so as to allow this patch to resonate at 5.45 GHz. The results of this study are illustrated in the reflection coefficient plots shown in Figure 8. The study demonstrate that the resonance frequency is reduced by increasing the dimension of the major or axis (Figure 6(a)), while reducing the dimension of the minor axis Y_e (Figure 6(b)).

Figure 7 illustrates the front and back views of the proposed microwave patch module with all dimensions labeled. Table 4 gives the front view dimensions of the designed microwave band patch antenna module while table 5 gives the back view dimensions of the module. The overall size of the antenna is 16×15 mm^2.

2) SIMULATION RESULTS

Figure 8 illustrates the frequency response of the gain, efficiency and VSWR respectively. It is clear that the gain is 2.45 dBi, efficiency is 0.77 and the VSWR value is 1.044 all at 5.45 GHz. This insures that the optimum values of these merits are obtained at the resonance frequency. Outside the bandwidth region (±0.5 GHz), these values start to drop significantly.

TABLE 4. Front view dimensions of the designed microwave band patch antenna module.

	Width (in mm)		Length (in mm)	
	Symbol	Value	Symbol	Value
patch	W_p	9.1	L_p	7.3
Feedline	W_f	2.519	L_f	5
Right Inset	X_{in}	0.25	Y_{in}	5.2
Left Inset	X_{in}	0.25	Y_{in}	5.2
Left slot	W_{Slot}	1.5	L_{Slot}	4.3
Right slot	W_{Slot}	1.5	L_{Slot}	4.3

TABLE 5. Back view dimensions of the designed microwave band patch antenna module.

	Width (in mm)		Length (in mm)	
Ground	W_s	16	L_s	15
DGS	Major axis		Minor Axis	
	X_e	15.35	Y_e	4.8

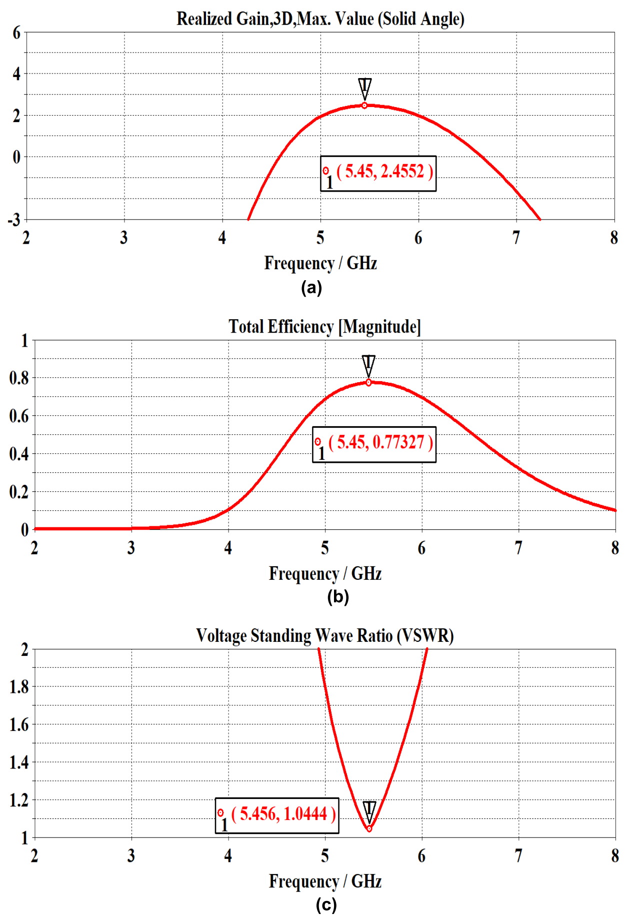

FIGURE 8. Frequency response of the proposed microwave patch antenna modules (a)Gain (b) Efficiency (c) VSWR.

The radiation patterns of the proposed module are illustrated in Figure 9. The E- and H- plane plots are shown in Figure 9(a) at three frequencies, namely 4.95 GHz, 5.45 GHz and 6 GHz. It is quite notable that the far field pattern is not much affected if the frequency deviates from the resonance

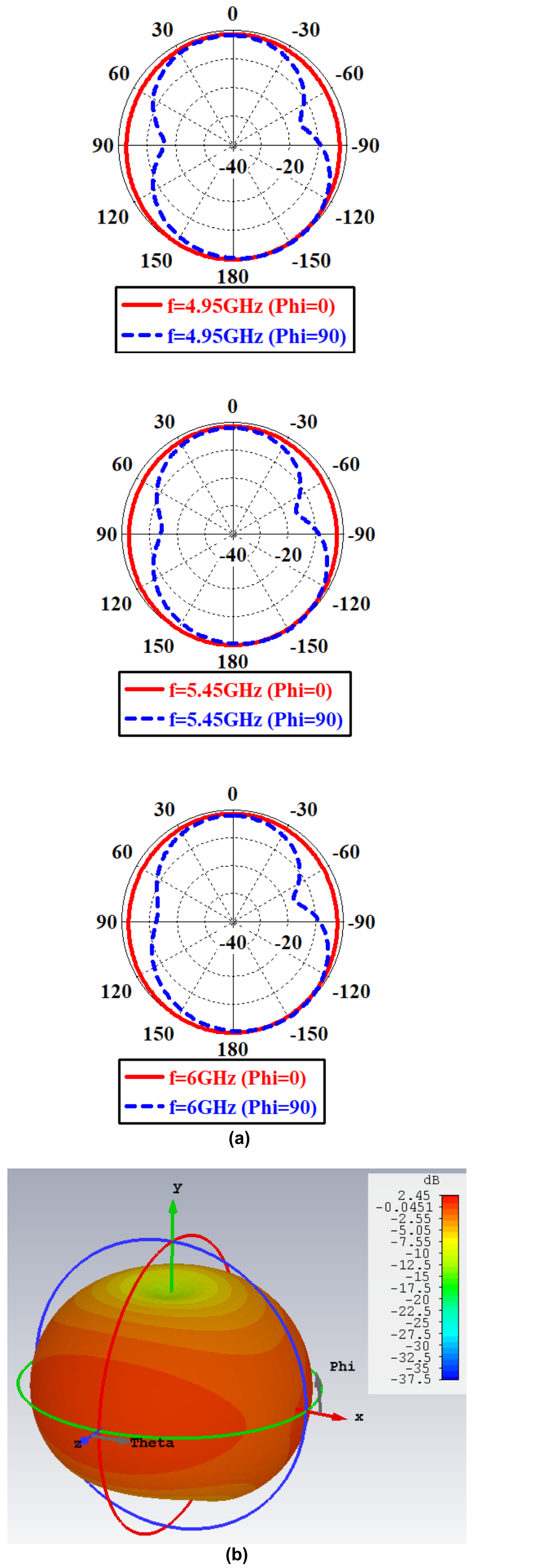

FIGURE 9. The radiation pattern of the proposed microwave antenna patch module (a) E- and H- plane plots (b) 3-D plot at resonance frequency.

one within the bandwidth limits. It is clear the proposed design exhibits omnidirectional pattern in H-plane when $\varphi = 0\,^{o}$ and at the H-plane is has a figure of eight pattern

TABLE 6. Comparisons between the parameter values of the proposed microwave patch and different designs available in literature.

Parameter Ref. No.	Resonance frequency (GHz)	Size (mm)	Gain (dBi)	BW (GHz)	Return loss (dB)
[34]	2.5 5.8	44 × 41	1.37 3.9	.1 .2	-29.9 -15.16
[35]	5	60 × 50	5.295		-28.35
[36]	5 6	26 × 24	2.86	.4	-35.47
[28]	5.4	27.5 × 27.5	5.012	2.02%	-47.27
Proposed	5.45	16 × 15	2.45	1.12	-33.26

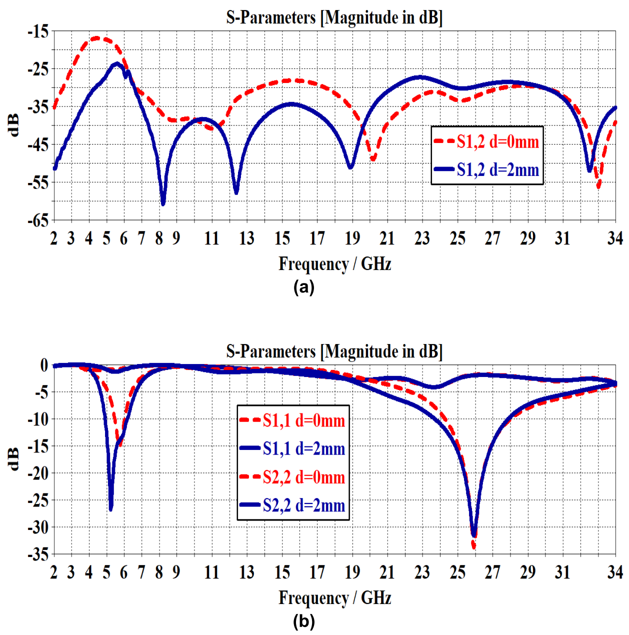

FIGURE 10. The effect of the fully connected gap and that isolated by 2mm gap for the (a) isolation parameter s21 (b) return-loss.

TABLE 7. Comparisons between the parameter values of the proposed compact and integrated microstrip antenna modules and different designs available in literature.

Parameter Ref. No	Resonance Frequency (GHz)	Size (mm^2)	Isolation (dB)
[16]	2.4, 5.5 and 28 GHz	45 × 40 × 0.508 mm^3	
[19]	21.6 27.6	60 × 100	15 25
[20]	3.8 & 5.5 26.85	110 × 75	43
[21]	from 1.7 to 3 from 25 to 38	110× 75	30
[22]	2.5 & 3.5 27 & 31	63× 5.6 28.3× 5.6 (orthogonal)	25
Proposed	5.4 25.75	24 × 15	26

(like dipole antenna) when $\varphi = 90\,^{o}$. The plot of the 3-D radiation pattern at 5.45 GHz is shown in Figure 9(b).

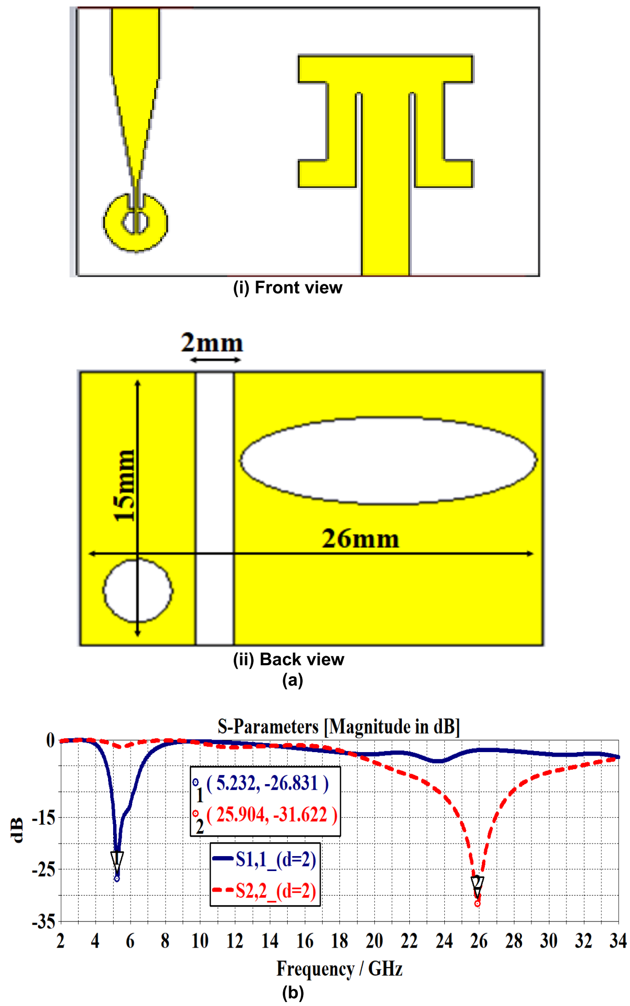

FIGURE 11. The structure of the proposed dual band antenna (a) Structure front and back view (b) Return loss of the proposed integrated structure.

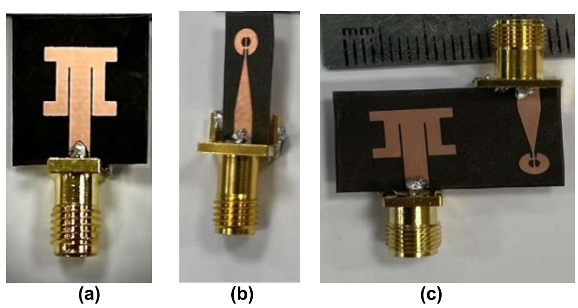

FIGURE 12. The fabricated proposed dual band antenna (a) The microwave patch module (b) The mm-Wave patch module (c) The integrated structure.

Table 6 gives a comparison between the parameter values of the proposed microwave patch and different designs available in literature. It is clear that the proposed design has the smallest size among them while keeping comparable values of other performance parameters.

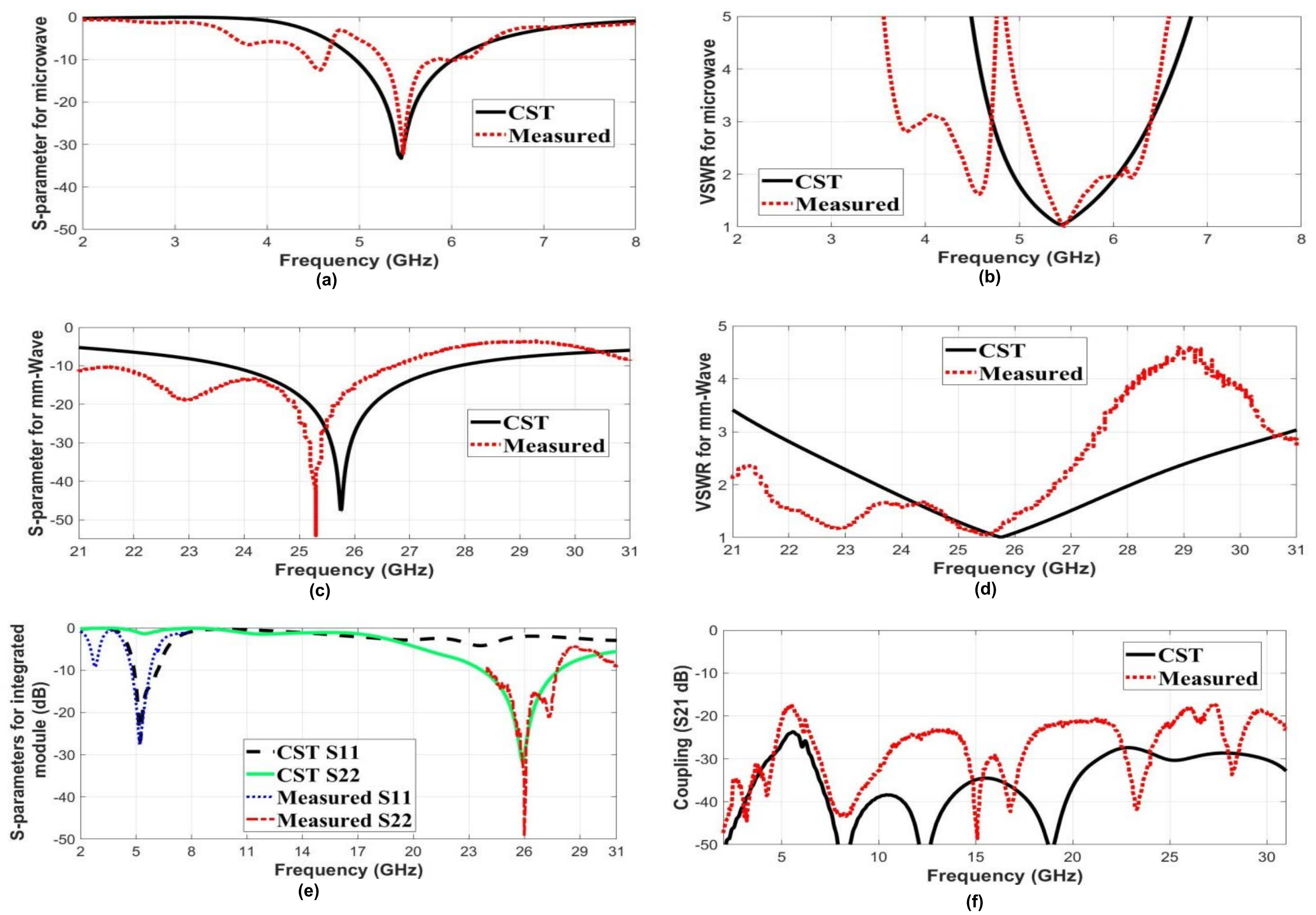

FIGURE 13. Comparisons of the practical measurements with the simulated ones of the proposed design (a) The microwave patch antenna module return loss (b) The microwave patch antenna module VSWR (c) The mm-Wave patch antenna module return loss (d) The mm-Wave patch antenna module VSWR (e) The compact and integrated microstrip antenna modules (f) The coupling between the compact and integrated microstrip antenna modules.

C. TWO DIFFERENT ANTENNA MODULES AT TWO DIFFERENT BANDS STRUCTURE

In this stage, the two previously designed antennas modules are integrated in on structure. A common substrate is used on which the two antennas are etched on the same side but with opposite directions to minimize the size of the structure from one hand, and to offer some degree of isolation between them on the other hand. However, it is necessary to ensure the highest degree of isolation between them. For this reason, a separating gap is introduced in the ground plane between the two antenna modules. Figure 10 shows the isolation parameter S12 at different values of the gap width d. It is clear that the case of d=2mm is better than that of the case of d=0 (no gap) at the microwave band. However, no much improvement is obtained in the mmWave band. This is because the wavelength of the resonance frequency in the microwave band is comparable to the ground plane length dimension, hence coupling is more significant. On the other hand, the wavelength of the resonance frequency at the mmWave band is less than that of the length of the ground plane, hence coupling is less significant. The opposite mounting of the two antennas minimizes the effect of coupling between the outer connectors (the coaxial cables) due to leakage currents. Also figure (10-b) shows the effect of the isolation on the return loss parameter.

The final proposed structure is shown in Figure 11(a) with an overall size of 24 x 15 mm^2 while the plot of the return loss for the complete structure is shown in Figure 11(b). It is clear that the performance does not differ than those of the case of separate antennas. The antenna structure still resonates at the two required frequencies of the microwave and mm-Wave bans with deep nulls obtained (less than -25 dB).

A comparison between the parameters values of the proposed compact and integrated microstrip antenna modules with other structures having integrated two different antennas available in literature are given in Table 7. The proposed structure has the smallest size as a trade off with the operating frequencies. It also exhibits a fairly good degree of isolation between the two antenna ports.

IV. PRACTICAL MEASUREMENTS

The proposed antenna structure is implemented using Rogers RT5880 substrate. Each antenna has been tested separately using the vector network analyzer (ROHDE & SCHWARZ

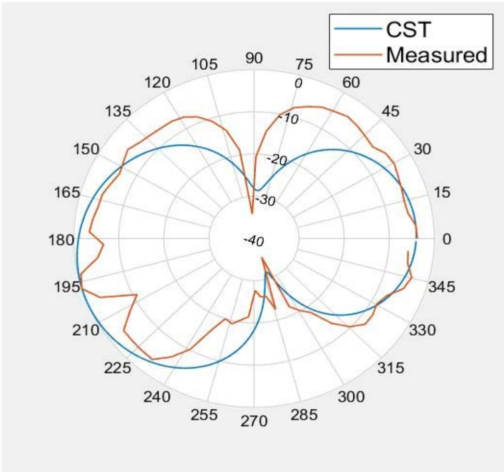

(a)

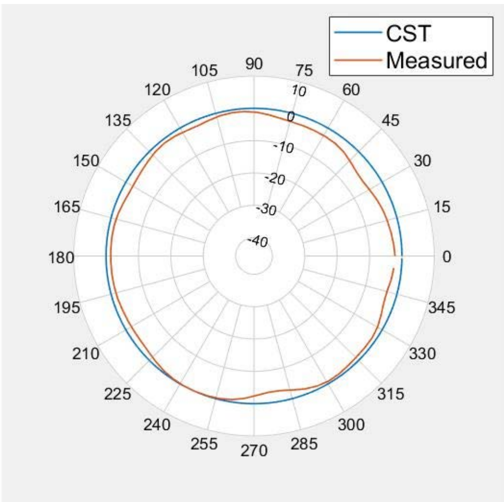

(b)

FIGURE 14. Measured and simulated radiation patterns of the proposed microwave patch module (a) E-plane (b) H-plane.

ZVA 67), and then the integrated antennas are tested with the same analyzer. The microwave antenna is connected with SMA connector while the mm-Wave antenna is connected with SMA KS-T08 connector with Φ 0.5mm rear socket pin inside and PCB thickness 0.8mm.

The fabricated antennas are shown in Figure 12 while the experimental results of the return loss as compared with simulated ones are shown in Figure 13. As can be observed, there is a high degree of agreement between simulated results and practical measurements.

The radiation pattern of the proposed microwave patch module is tested inside an anechoic chamber. A plot of the E-plane and H- plane patterns are shown in Figure 14 as comparted with the simulated one at 5.4 GHz. It is clear that the simulated and measured radiation patterns approximately have same shape with same locations of peaks and nulls.

Some pictures of the practical measurements setup are shown in Figure 15 as well as the device's model.

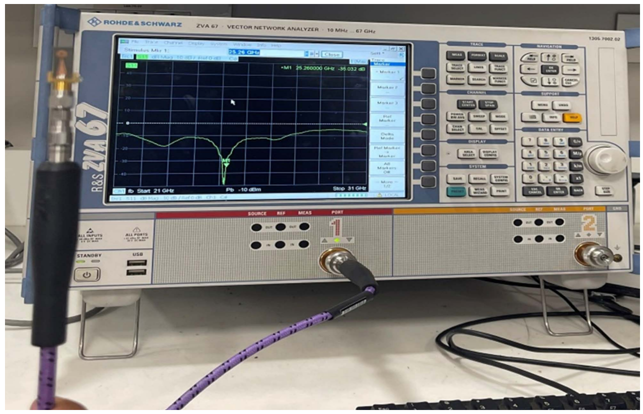

(a)

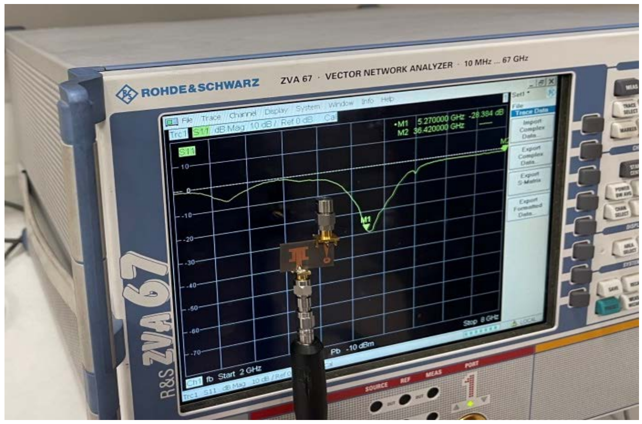

(b)

FIGURE 15. Measured setup (a) single mm-wave antenna (b) integrated microwave antenna.

V. CONCLUSION

The introduction of the millimeter-wave (mm-Wave) frequency bands along with the microwave band in communication systems, made it necessary to propose new designs of antennas that can cope with the two bands while keeping the sizes as small as possible. The current work presented a design, simulation and practical implementation, of two different antenna modules at two different bands integrated on one structure in which the miniaturized size was the main objective to achieve. The proposed structure was based on two separate modules designed under dimensions constraint. The practical measurements were in good agreement with the simulated ones. On the other hand, main objective of the design was achieved as illustrated in the comparison with other designs available in literature. The proposed structure is suitable for 5G systems where the allocated frequency bands lie within the range of the operating frequencies of the structure. On the other hand, it is most suitable being used in miniaturized devices utilized in applications such as the Internet of Things (IoT). The proposed antenna structure can operate in two of the assigned 5G bands, namely the sub-6 GHz (0.41 GHz to 7.125 GHz) and the mmWave (24.25 GHz to 52.6 GHz) according to the 3GPP. The sub-6 GHz band is suited for mobile communications and WiFi, while the mm-wave band is suited for applications that require high data rates but in limited regions such as IoT

REFERENCES

[1] R. Rashmitha, N. Niran, A. A. Jugale, and M. R. Ahmed, "Microstrip patch antenna design for fixed mobile and satellite 5G communications," in *Proc. 3rd Int. Conf. Comput. Netw. Commun. (CoCoNet)*, 2019, pp. 2073–2079.

[2] S. Kumar, S. A. Dixit, R. R. Malekar, D. H. Raut, and K. L. Shevada, "Fifth generation antennas: A comprehensive review of design and performance enhancement techniques," *IEEE Access*, vol. 8, pp. 163568–163593, 2020.

[3] M. Abirami, "A review of patch antenna design for 5G," in *Proc. IEEE Int. Conf. Electr., Instrum. Commun. Eng. (ICEICE)*, Apr. 2017, pp. 1–3.

[4] M. H. Sharaf, A. I. Zaki, R. K. Hamad, and M. M. M. Omar, "A novel dual-band (38/60 GHz) patch antenna for 5G mobile handsets," *Sensors*, vol. 20, no. 9, p. 2541, 2020.

[5] S. R. Thummaluru and R. R. K. Chaudhary, "Isolation and frequency reconfigurable compact MIMO antenna for wireless local area network applications," *IET Microw., Antennas Propag.*, vol. 13, no. 4, pp. 519–525, 2019.

[6] R. Mittra, "Some challenges in millimeter wave antenna designs for 5G," in *Proc. Int. Symp. Antennas Propag. (ISAP)*, 2018, pp. 1–2.

[7] C. C. Chan, F. G. Kurnia, A. Al-Hournani, K. M. Gomez, S. Kandeepan, and W. Rowe, "Open-source and low-cost test bed for automated 5G channel measurement in mmWave band," *J. Infr., Millim., THz Waves*, vol. 40, no. 5, pp. 535–556, May 2019.

[8] V. Waladi, N. Mohammadi, Y. Zehforoosh, A. Habashi, and J. Nourinia, "A novel modified star-triangular fractal (MSTF) monopole antenna for super-wideband applications," *IEEE Antennas Wireless Propag. Lett.*, vol. 12, pp. 651–654, 2013.

[9] B. L. Shahu, S. Pal, and N. Chattoraj, "A compact super wideband monopole antenna design using fractal geometries," *Microw. Rev.*, vol. 20, no. 2, pp. 20–24, Dec. 2014.

[10] S. Das, D. Mitra, and R. B. S. Chaudhuri, "Staircase fractal loaded microstrip patch antenna for super wide band operation," *Prog. Electromagn. Res. C*, vol. 95, pp. 183–194, 2019.

[11] N. Sharma, S. S. Bhatia, and V. Sharma, "Peano–Gosper, Koch and Minkowski fractal curvesbased novel hybrid antenna using modified partial ground plane for multi-standard wireless applications," *J. Electromagn. Waves Appl.*, vol. 35, no. 15, pp. 1959–1979, 2021.

[12] A. Gupta and P. Chawla, "Review on fractal antenna: Inspiration through Nature," *Int. J. Sci. Eng. Appl. Sci.*, vol. 1, no. 4, pp. 1–7, Jun. 2015.

[13] P. Singh and R. Scholar, "Application of fractal antennas with advantages and disadvantages," *Int. J. Creative Res. Though*, vol. 6, no. 2, pp. 1–4, Apr. 2018.

[14] S. Singhal and K. A. Singh, "CPW-fed Phi-shaped monopole antenna for super-wideband application," *Prog. Electromagn. Res. C*, vol. 64, pp. 105–116, 2016.

[15] J. Saini and K. M. Garg, "PBG structured compact antenna with switching capability in lower and upper bands of 5G," *Prog. Electromagn. Res. M*, vol. 94, pp. 19–29, 2020.

[16] E. M. Yassin, A. H. Mohamed, A. F. E. Abdallah, and S. H. El-Hennawy, "Single-fed 4G/5G multiband 2.4/5.5/28 GHz antenna," *IET Microw., Antennas Propag.*, vol. 13, no. 3, pp. 286–290, 2019.

[17] C. Liu, Y. Chen, D. Yang, and Z. Tu, "A planar single-port dual-band antenna using small ground with LFR," in *Proc. 9th Asia–Pacific Conf. Antennas Propag. (APCAP)*, 2020, pp. 1–2.

[18] M. Ikram, N. Nguyen-Trong, and A. M. Abbosh, "Realization of a tapered slot array as both decoupling and radiating structure for 4G/5G wireless devices," *IEEE Access*, vol. 7, pp. 159112–159118, 2019.

[19] R. Hussain, A. T. Alreshaid, S. K. Podilchak, and M. S. Sharawi, "Compact 4G MIMO antenna integrated with a 5G array for current and future mobile handsets," *IET Microw., Antennas Propag.*, vol. 11, no. 2, pp. 271–279, Jan. 2017.

[20] I. S. Naqvi, H. A. Naqvi, F. Arshad, A. M. Riaz, A. M. Azam, S. M. Khan, Y. Amin, J. Loo, and A. H. Tenhunen, "An integrated antenna system for 4G and millimeter-wave 5G future handheld devices," *IEEE Access*, vol. 7, pp. 116555–116566, 2019.

[21] I. M. Magray, S. G. Karthikeya, K. Muzaffar, and K. S. Koul, "Corner bent integrated design of 4G LTE and mm-wave 5G antennas for mobile terminals," *Prog. Electromagn. Res.*, vol. 84, pp. 167–175, 2019.

[22] A. S. Malik, K. Muzaffar, H. A. Mir, and H. A. Moon, "Extremely close integration of dual band sub-6 GHz 4G antenna with unidirectional mm-wave 5G antenna," *Prog. Electromagn. Res. Lett.*, vol. 96, pp. 73–80, 2021.

[23] J. Chatterjee, A. Mohan, and V. Dixit, "Broadband circularly polarized H-shaped patch antenna using reactive impedance surface," *IEEE Antennas Wireless Propag. Lett.*, vol. 17, no. 4, pp. 625–628, Apr. 2018.

[24] M. T. I.-u. Huque, M. Chowdhury, M. K. Hosain, and M. S. Alam, "Performance analysis of corporate feed rectangular patch element and circular patch element 4×2 microstrip array antennas," *Int. J. Adv. Comput. Sci. Appl.*, vol. 2, no. 7, pp. 16–21, 2011.

[25] N. Kumar, K. K. Singh, and R. K. Badhai, "A tapered feed circular monopole super ultra-wideband (UWB) printed antenna," in *Proc. Int. Conf. Commun. Signal Process. (ICCSP)*, Melmaruvathur, India, Apr. 2016, pp. 6–8.

[26] J. Liang, C. C. Chiau, X. Chen, and C. G. Parini, "Printed circular disc monopole antenna for ultrawide band applications," *Electron. Lett.*, vol. 40, no. 20, pp. 1246–1247, Sep. 2004.

[27] C. A. Balanis, *Antenna Theory Analysis And Design*, 3rd ed. Hoboken, NJ, USA: Wiley, 2005.

[28] M. Z. Rahman, K. C. D. Nath, and M. Mynuddin, "Performance analysis of an inset-fed circular microstrip patch antenna using different substrates by varying notch width for wireless communications," *Int. J. Electromagn. Appl.*, vol. 10, no. 1, pp. 19–29, 2020.

[29] S. Dichi, R. Suci, and W. Putri, "An improved design of multiband patch antenna at 26 GHz for 5G mobile," in *Proc. Int. Conf. Eng. Inf. Technol. Sustain. Ind. (ICONETSI)*, 2020, pp. 1–5.

[30] Gunaram, V. Sharma, S. Shekhawat, P. Jain, and J. K. Deegwal, "Elliptical slot embedded monopole circular patch antenna for 5G applications," in *Proc. 3rd Int. Conf. Condens. Matter Appl. Phys. (ICC)*, 2019, Art. no. 130073.

[31] J. Colaco and R. Lohani, "Design and implementation of microstrip circular patch antenna for 5G applications," in *Proc. Int. Conf. Electr., Commun., Comput. Eng. (ICECCE)*, Jun. 2020, pp. 1–4.

[32] M. M. Kamal, S. Yang, S. H. Kiani, M. R. Anjum, M. Alibakhshikenari, Z. A. Arain, A. A. Jamali, A. Lalbakhsh, and E. Limitim, "Donut-shaped mm-Wave printed antenna array for 5G technology," *Electronics*, vol. 10, no. 12, p. 1415, 2021.

[33] H. H. Ghouz, "Novel compact and dual-broadband microstrip MIMO antennas for wireless applications," *Prog. Electromagn. Res. B*, vol. 63, pp. 107–121, 2015.

[34] R. S. Uqaili, J. A. Uqaili, S. Zahra, F. B. Soomro, and A. Akbar, "A study on dual-band microstrip rectangular patch antenna for Wi-Fi," *Proc. Eng. Technol. Innov.*, vol. 16, pp. 1–2, Aug. 2020.

[35] S. Khilariwal, R. Verma, and M. D. Upadhayay, "Design of notch antenna for 5 GHz high speed LAN," in *Proc. Int. Conf. Wireless Commun., Signal Process. Netw. (WiSPNET)*, Mar. 2016, pp. 999–1002.

[36] A. Abhishek and P. Suraj, "Design of patch antenna for 5G communication at 6 GHz (WRC-23) with WLAN application," in *Proc. 6th Int. Conf. Converg. Technol. (ICT)*, Apr. 2021, pp. 1–5.

[37] R. Dilli, "Analysis of 5G wireless systems in FR1 and FR2 frequency bands," in *Proc. 2nd Int. Conf. Innov. Mech. Ind. Appl. (ICIMIA)*, Mar. 2020, pp. 767–772.

MARWA M. EL-WAZZAN was born in Cairo, Egypt, in 1991. She received the B.S. degree from the Arab Academy for Science and Technology and Maritime Transport, Cairo, in 2013. Her research interests include antenna design and mobile communication systems.

HUSSEIN H. GHOUZ was born in Alexandria, Egypt, in 1959. He received the B.Sc. and M.Sc. degrees (Hons.) in radar communication systems engineering from the Military Technical College (MTC), Cairo, Egypt, in 1983 and 1990, respectively, and the Ph.D. degree in electrical engineering from Arizona State University, Tempe, in 1996. He was a Lecturer with the Department of Electronic Warfare Engineering (EWE), MTC, from 1997 to 2010. In 2011, he joined the Department of Communications Engineering, Arab Academy for Science, Technology and Maritime Transport (AASTMT), as an Associated Professor. He has been a Full Professor in communications engineering, AASTMT, since 2017. His research interests include modeling and design of flip chip interconnects in passive MMIC circuits' applications, planner antennas, numerical techniques, adaptive space-time filtering techniques, and anti-jamming techniques in radar systems. He is a member of the IEEE Microwave Theory and Technique Society and the IEEE Signal Processing Society.

SHERIF K. EL-DIASTY received the B.Sc. and M.Sc. degrees from the Arab Academy for Science, Technology and Maritime Transport (AASTMT), Cairo, Egypt, in 1998 and 2006, respectively, and the Ph.D. degree from Ain Shams University, Cairo, in 2018, all in electrical engineering (electronics and communications). He is currently an Assistant Professor with the Department of Electronics, AASTMT.

MOHAMED A. ABOUL-DAHAB (Life Senior Member, IEEE) received the B.Sc. degree in communication engineering from the Faculty of Engineering, Cairo University, in 1973, and the M.Sc. and Ph.D. degrees in communication engineering from Alexandria University, Egypt, in 1980 and 1986, respectively. He was the Head of the Department Electronics and Computer Engineering, from 1995 to 2002, and the Dean of the College of Engineering and Technology, Arab Academy for Science, Technology and Maritime Transport (AASTMT), Cairo, Egypt, from 2002 to 2008. He has been a Professor of communications engineering with AASTMT, since 1999. His publications are in the areas of antennas, channel coding, and wireless networks, in addition to some publications in the field of education. He was a member of the National Radio Science Committee, from 1993 to 2015, and the Chairperson of the National Committee for the Information and Communication Technology (ICT), from 2015 to 2021; both are belonging to the Academy of Scientific Research and Technology.